

## Physicochemical Interpretation, with QSAR/SAR Analysis, of How the Barriers of *Pseudomonas Aeruginosa* Bacteria were Penetrated by *Para*-Substituted *N*-Arylbenzylimines: Synthesis, Characterization, and *In Vitro* Antibacterial Effect

Delia Quintana-Zavala<sup>1</sup>, Jessica Rubí Morán-Díaz<sup>1,5</sup>, José Luis Ávila-Melo<sup>2</sup>, Raquel Gómez-Pliego<sup>3</sup>, Hugo Alejandro Jiménez-Vázquez<sup>2</sup>, José Guadalupe Trujillo-Ferrara<sup>4\*</sup>, Juan Alberto Guevara-Salazar<sup>5\*</sup>

<sup>1</sup>Laboratorio de Química Orgánica, Centro de Investigación en Ciencia Aplicada y Tecnología Avanzada, Unidad Legaria, Instituto Politécnico Nacional, Legaria No. 694, C.P. 11500, CDMX.

<sup>2</sup>Departamento de Química Orgánica, Escuela Nacional de Ciencias Biológicas, Instituto Politécnico Nacional, Prolongación Manuel Carpio y Plan de Ayala, Col. Plutarco Elías Calles, Alcaldía Miguel Hidalgo, C.P. 11350, CDMX.

<sup>3</sup>Sección de Ciencias Biológicas y de la Salud, Departamento de Ciencias Biológicas, Facultad de Estudios Superiores Cuautitlán, Universidad Nacional Autónoma de México, Av. 1 de Mayo s/n, Santa María las Torres, Cuautitlán Izcalli, C.P. 54740, México.

<sup>4</sup>Laboratorio de Bioquímica Médica, Sección de estudios de Posgrado e Investigación. Escuela Superior de Medicina, Instituto Politécnico Nacional, Plan de San Luis y Díaz Mirón, S/N, Col. Santo Tomas, Alcaldía Miguel Hidalgo, C.P. 11340, CDMX.

<sup>5</sup>Departamento de Farmacología. Escuela Superior de Medicina, Instituto Politécnico Nacional, Plan de San Luis y Díaz Mirón, S/N, Col. Santo Tomas, Alcaldía Miguel Hidalgo, C.P. 11340, CDMX.

**\*Corresponding author:** José Guadalupe Trujillo-Ferrara, email: [jtrujillo@ipn.mx](mailto:jtrujillo@ipn.mx); Phone/fax: +52 (55) 57296000, ext. 62747, Juan Alberto Guevara-Salazar, email: [jguevaras@ipn.mx](mailto:jguevaras@ipn.mx); Phone/fax: +52 (55) 57296000, ext. 62788.

Received December 7<sup>th</sup>, 2020; Accepted April 27<sup>th</sup>, 2021.

DOI: <http://dx.doi.org/10.29356/jmcs.v65i3.1481>

**Abstract.** Resistance to antibiotics is a growing problem that imposes limitations on current therapy around the world. The World Health Organization (WHO) recommends creating new antibacterial molecules to inhibit the most harmful bacteria by aiming at specific targets. Among such bacteria is multi-drug resistant *Pseudomonas aeruginosa*, a Gram-negative bacterium responsible for 70% of invasive infections worldwide. The aim of this investigation was to synthesize *N*-arylbenzylimines, examine their antibacterial activity against *P. aeruginosa* ATCC 27853, and determine their physicochemical properties by quantitative structure-activity relationship (QSAR/SAR) analysis. Seven *N*-arylbenzylimines were synthesized with yields  $\geq 50\%$ , all with the *E*-configuration (as shown by NMR spectra and confirmed with X-ray diffraction). The *in vitro* microbiological evaluations were carried out with the Kirby-Bauer method, following the guidelines of the Clinical & Laboratory Standards Institute (CLSI). The *N*-arylbenzylimines produced a very good antibacterial effect on *P. aeruginosa*, with minimum inhibitory concentration (MIC) values ranging from 198.47-790.10  $\mu\text{M}$ , calculated by the Hill method. Based on the slopes of the concentration-response curves, the mechanism of action is different between the test compounds and aztreonam, the reference drug. The QSAR study performed with *in vitro* experimental data found that biological activity correlates most significantly with molecular size, followed

by lipophilicity and electronic effects. According to the SAR analysis of antibacterial activity, molecules cross bacterial barriers differently if they bear substituents with resonance versus inductive electronic effects. The physicochemical data presently described are of utmost importance for designing and developing new molecules to combat the pathogenicity and resistance of *P. aeruginosa*.

**Keywords:** Antibacterial activity; *E*-configuration; partition coefficient; electronic effects; QSAR/SAR.

**Resumen.** La resistencia a los antibióticos es un problema en aumento que impone limitaciones en la terapia actual a nivel mundial. La Organización Mundial de la Salud (OMS) recomienda crear nuevas moléculas antibacterianas para inhibir las bacterias más dañinas por medio de dianas específicas. *Pseudomonas aeruginosa*, entre estas bacterias, es Gram-negativa, resistente a múltiples fármacos, y responsable del 70% de las infecciones invasivas en el mundo. El objetivo de esta investigación fue sintetizar *N*-arilbenziliminas, examinar su actividad antibacteriana contra *P. aeruginosa* ATCC 27853, y determinar sus propiedades fisicoquímicas mediante análisis cuantitativo de relación estructura-actividad (QSAR/SAR). Todos los siete *N*-arilbenziliminas sintetizados tuvieron rendimientos  $\geq 50\%$  y la configuración *E* (de acuerdo con la espectroscopía de RMN y la difracción de rayos-X). Las pruebas microbiológicas *in vitro* se realizaron mediante el método Kirby-Bauer, siguiendo las directrices del Instituto de Estándares Clínicos y de Laboratorio (CLSI). Las *N*-arilbenziliminas mostraron efecto antibacteriano relevante sobre *P. aeruginosa*, con valores de la concentración mínima inhibitoria (MIC) en el rango de 198.47-790.10  $\mu\text{M}$ , calculado por el método de Hill. Las pendientes de las curvas de concentración-respuesta sugieren que el mecanismo de acción es distinto entre las *N*-arilbenziliminas y aztreonam, el fármaco de referencia. El análisis QSAR de los datos experimentales indica que la actividad biológica se correlaciona de manera más significativa con el tamaño molecular, seguida de la lipofiliidad y los efectos electrónicos. Según el análisis SAR de la actividad antibacteriana, las moléculas cruzan las barreras bacterianas en forma diferente si portan sustituyentes con efectos electrónicos inductivos versus de resonancia. Estos datos fisicoquímicos son de suma importancia en el diseño y desarrollo de nuevas moléculas para combatir la infección y resistencia de *P. aeruginosa*.

**Palabras clave:** Actividad antibacteriana; configuración *E*; coeficiente de partición; efectos electrónicos; QSAR/SAR

---

## Introduction

Although substituted *N*-arylbenzylimines have been investigated as antibacterial and antifungal molecules [1-3], little is known about their possible mechanism of action for inhibiting bacterial growth. According to the World Health Organization (WHO), it is important to design and develop compounds directed at specific targets in bacteria and determine the antibacterial mechanism of action involved [4]. Thus, the priority is to find molecules that can inhibit the bacteria most harmful to the world population and that do so with mechanisms of action distinct from those of current clinical drugs [5-8].

The bacteria responsible for the most lethal communicable diseases are *Acinetobacter*, *Pseudomonas*, *Klebsiella*, *Escherichia coli*, *Serratia*, *Staphylococcus aureus* and *Proteus* [9, 10]. They trigger local and systemic diseases such as soft-tissue infections, pneumonia, meningitis, sepsis, septic shock, and multiple organ failure. Multidrug-resistant *Pseudomonas aeruginosa*, responsible for 70% of invasive infections, induces hospital infections and sepsis [11].

An imine, or Schiff base, is formed by the reaction of ammonia or a primary amine with an aldehyde or ketone [12]. Similar to alkenes, Schiff bases can express *syn/anti* (*Z/E*) isomerism in the C=N double bond [13, 14], which is a useful property for catalytic processes [15, 16], organic synthesis, and the formation of metal complexes [17].

The aim of the current study was to synthesize seven *N*-arylbenzylimines, evaluate their antibacterial activity *in vitro* on *P. aeruginosa*, and carry out a quantitative structure-activity relationship (QSAR) analysis, considering lipophilicity as well as the electronic and steric effects proposed by Hansch-Fujita. The *N*-arylbenzylimines synthesized and tested against *P. aeruginosa* are structurally very similar. The common skeleton of *N*-aryl-arylmethyleneimines [18-23] was strategically substituted in the *para* position with different

electron donating and withdrawing groups, and then characterized spectroscopically. NMR spectra and X-ray diffraction showed that all seven synthesized compounds had an *E*-configuration. Biological activity was examined *in vitro* by the agar diffusion method (Kirby-Bauer), and the MIC was calculated with the Hill method.

## Experimental

### *In silico* study

#### Evaluation of the ADMET properties

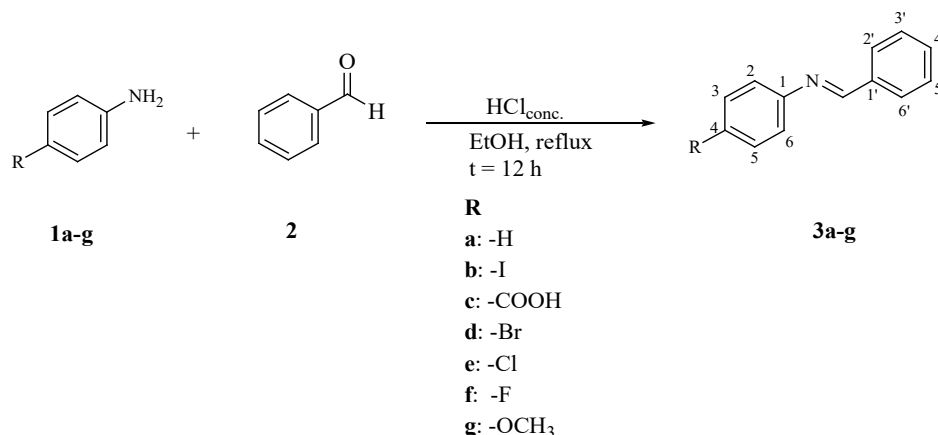
By utilizing the admetSAR (version 2.0) [24, 25], SwissADME [26-29], SMARTCyp [30-32] and MarvinSketch 6.0.0 [33] bioinformatic server, the physicochemical ADMET properties (absorption, distribution, metabolism, excretion and toxicity) of the seven *N*-arylbenzylimines herein synthesized were theoretically calculated and related to their pharmacodynamic behavior. An in-depth comparison of the structural characteristics of the test compounds was made by running experimental values obtained from similar known compounds in the corresponding software, and acute and chronic toxicity were estimated [24, 25].

#### Materials and methods

All reagents and solvents were used as received from Sigma-Aldrich®. Thin-layer chromatography (TLC) was performed with Merck-DC-F254® silica gel on aluminum plates and revealed with a short-wave UV lamp at  $\lambda = 254$  nm. Melting points were determined on a Mel-Temp apparatus (Laboratory Devices Inc., USA). IR spectra were recorded on a Pike Technologies GladiATR spectrophotometer and UV-Vis spectra on a Beckman Coulter DU 650 spectrophotometer.  $^1\text{H}$ ,  $^{13}\text{C}$ , NOE and HSCQ NMR spectra were acquired on a Varian VNMR-500 spectrometer at 500 MHz and a Bruker Avance spectrometer at 600 MHz (125.8 and 150.9 MHz for  $^{13}\text{C}$ , respectively) in  $\text{CDCl}_3$ , using TMS as internal reference. Chemical shifts ( $\delta$ ) are reported in parts per million (ppm). Coupling constants ( $J$ ) are given in Hz. High-resolution electrospray ionization mass spectrometry (ESI-MS) was performed with an Agilent 6545 Q-TOF LC/MS instrument. Chemical purity was examined by high-performance liquid chromatography (HPLC) with an Agilent 1200 Infinity Series apparatus.

#### Synthesis and characterization

Equimolar amounts of the corresponding *para*-substituted anilines (**1a-g**) and benzaldehyde (**2**) diluted in 60 mL of ethanol were put in a round-bottom flask. The reaction was carried out in an acidic medium (with concentrated HCl as the catalyst) and left under reflux for 12 h. Subsequently, recrystallization was achieved by evaporating the solvent and placing the reaction crude in an ice bath [34-35]. The product was filtered under vacuum and purified by sublimation (Scheme 1).



**Scheme 1.** The method of preparation for (*E*) *N*-arylbenzylimines.

**(E)-1-(N-phenyl)-1-phenylmethanimine (3a)**

A yellow solid was obtained in 80% yield; mp 48-50 °C;  $R_f$  0.86 (*n*-hexane/AcOEt 7: 3); UV-Vis (MeOH)  $\lambda_{\max}$  = 267.8  $\pm$  3.5 nm,  $\epsilon$  = 135500 mol<sup>-1</sup>·dm<sup>3</sup>·cm<sup>-1</sup>; IR = 1574.97 (-C=N-), 3059.43, 1480.92, 1448.20 (aromatic) cm<sup>-1</sup>; <sup>1</sup>H NMR (CDCl<sub>3</sub>, 600 MHz):  $\delta$  = 8.53 (-HC=N-, 1H, s), 7.99 (H2', H6', 2H, d, <sup>3</sup>J<sub>H-H</sub> = 8.4 Hz), 7.56-7.55 (H3', H4', H5', 3H, m), 7.48 (H2, H6, 2H, d, <sup>3</sup>J<sub>H-H</sub> = 7.8 Hz), 7.32-7.29 (H3, H4, H5, 3H, m); <sup>13</sup>C NMR (CDCl<sub>3</sub>, 150 MHz):  $\delta$  = 160.4 (-HC=N-), 152.1 (C-1), 136.2 (C-1'), 131.4 (C-4'), 129.1, (C-2, C-6), 128.8 (C-2', C-6'), 128.8 (C-3', C-5'), 125.9 (C-4), 120.9 (C-3, C-5); EIMS  $m/z$  [M+H]<sup>+</sup> 182.09 (calcd. 181.09).

**(E)-1-[N-(4-iodophenyl)]-1-phenylmethanimine (3b)**

A bright grey solid was provided in 40% yield; mp 74-76 °C;  $R_f$  0.50 (*n*-hexane/AcOEt 7:3); UV-Vis (MeOH):  $\lambda_{\max}$  = 269.25  $\pm$  2.85 nm,  $\epsilon$  = 2002900 mol<sup>-1</sup>·dm<sup>3</sup>·cm<sup>-1</sup>; IR = 1569.90 (-C=N-), 3053.87, 1620.94, 1475.68, 1452.13 (aromatic), 529.55 (-C-I), 1958.53, 1903.60, 823.99 (*para*-substituted) cm<sup>-1</sup>; <sup>1</sup>H NMR (CDCl<sub>3</sub>, 600 MHz):  $\delta$  = 8.47 (-HC=N-, 1H, s), 7.95 (H2', H6', 2H, d, <sup>3</sup>J<sub>H-H</sub> = 7.80 Hz), 7.56-7.52 (H3', H4', H5', 3H, m), 7.76 (H3, H5, 2H, d, <sup>3</sup>J<sub>H-H</sub> = 7.80 Hz), 7.02 (H2, H6, 2H, d, <sup>3</sup>J<sub>H-H</sub> = 8.40 Hz); <sup>13</sup>C NMR (CDCl<sub>3</sub>, 150 MHz):  $\delta$  = 160.8 (-HC=N-), 151.7 (C-1), 138.1 (C-3, C-5), 137.9 (C-1'), 135.9 (C-4), 131.7 (C-4'), 128.9 (C-2', C-6'), 128.8 (C-3', C-5'), 123.0 (C-2, C-6); EIMS  $m/z$  [M+H]<sup>+</sup> 307.99 (calcd. 306.99).

**(E)-4-(N-methylenephénylimino)benzoic acid (3c)**

A white solid was afforded in 60% yield; mp 194-196 °C;  $R_f$  0.63 (*n*-hexane/AcOEt 7:3); UV-Vis (MeOH):  $\lambda_{\max}$  = 274.3  $\pm$  0.5 nm,  $\epsilon$  = 161740 mol<sup>-1</sup>·dm<sup>3</sup>·cm<sup>-1</sup>; IR = 1677.21 (-C=O- acid), 1574.97 (-C=N-), 3063.92, 1595.42, 1427.65 (aromatic), 851.15 (*para*-substituted) cm<sup>-1</sup>; <sup>1</sup>H NMR (DMSO, 500 MHz):  $\delta$  = 12.68 (-COOH, 1H, br), 8.63 (-HC=N-, 1H, s), 7.98 (H3, H5, 2H, d, <sup>3</sup>J<sub>H-H</sub> = 9.0 Hz), 7.95 (H2', H6', 2H, d, <sup>3</sup>J<sub>H-H</sub> = 8.0 Hz), 7.57-7.51 (H3', H4', H5', 3H, m), 7.316 (H2, H6, 2H, d, <sup>3</sup>J<sub>H-H</sub> = 8.50 Hz); <sup>13</sup>C NMR (DMSO, 125 MHz):  $\delta$  = 167.9 (-COOH), 167.4 (-HC=N-), 155.8 (C-1), 136.1 (C-1'), 135.0 (C-3, C-5), 131.0 (C-4'), 129.3 (C-2', C-6'), 129.3 (C-3', C-5'), 128.4 (C-2, C-6), 121.4 (C-4); EIMS  $m/z$  [M+H]<sup>+</sup> 226.08 (calcd. 225.08).

**(E)-1-[N-(4-bromophenyl)]-1-phenylmethanimine (3d)**

A bright grey solid was produced in 50% yield; 66-68 °C;  $R_f$  0.80 (*n*-hexane/AcOEt 7:3); UV-Vis (MeOH):  $\lambda_{\max}$  = 268.8  $\pm$  1.8 nm,  $\epsilon$  = 259520 mol<sup>-1</sup>·dm<sup>3</sup>·cm<sup>-1</sup>; IR = 1574.19 (-C=N-), 1619.96, 1480.92, 1399.13 (aromatic), 523.99 (-C-Br), 1888.62, 818.43 (*para*-substituted) cm<sup>-1</sup>; <sup>1</sup>H NMR (CDCl<sub>3</sub>, 600 MHz):  $\delta$  = 8.48 (-HC=N-, 1H, s), 7.95 (H2', H6', 2H, d, <sup>3</sup>J<sub>H-H</sub> = 7.8 Hz), 7.56-7.54 (H3', H4', H5', 3H, m), 7.56 (H3, H5, 2H, d, <sup>3</sup>J<sub>H-H</sub> = 8.4 Hz), 7.15 (H2, H6, 2H, d, <sup>3</sup>J<sub>H-H</sub> = 9.0 Hz); <sup>13</sup>C NMR (CDCl<sub>3</sub>, 150 MHz):  $\delta$  = 160.7 (-HC=N-), 151.0 (C-1), 135.9 (C-1'), 132.2 (C-3, C-5), 131.6 (C-4'), 128.9 (C-2', C-6'), 128.8 (C-3', C-5'), 122.6 (C-2, C-6), 119.3 (C-4); EIMS  $m/z$  [M+H]<sup>+</sup> 260.00 (calcd. 259.00).

**(E)-1-[N-(4-chlorophenyl)]-1-phenylmethanimine (3e)**

A bright yellow solid was furnished in 50% yield; 64-66 °C;  $R_f$  0.83 (*n*-hexane/AcOEt 7:3); UV-Vis (MeOH):  $\lambda_{\max}$  = 268.5  $\pm$  3.9 nm,  $\epsilon$  = 661250 mol<sup>-1</sup>·dm<sup>3</sup>·cm<sup>-1</sup>; IR = 1570.88 (-C=N-), 1619.96, 1468.65, 1452.29, 1399.13 (aromatic), 683.48 (-C-Cl), 1889.86, 818.43 (*para*-substituted) cm<sup>-1</sup>; <sup>1</sup>H NMR (CDCl<sub>3</sub>, 500 MHz):  $\delta$  = 8.34 (-HC=N-, 1H, s), 7.806 (H2', H6', 2H, d, <sup>3</sup>J<sub>H-H</sub> = 8.0 Hz), 7.40-7.38 (H3', H4', H5', 3H, m), 7.26 (H3, H5, 2H, d, <sup>3</sup>J<sub>H-H</sub> = 9.0 Hz), 7.06 (H2, H6, 2H, d, <sup>3</sup>J<sub>H-H</sub> = 9.0 Hz); <sup>13</sup>C NMR (CDCl<sub>3</sub>, 125 MHz):  $\delta$  = 160.9 (-HC=N-), 150.7 (C-1), 136.1 (C-1'), 131.8 (C-4'), 131.6 (C-4), 129.4 (C-3, C-5), 129.1 (C-2', C-6'), 129.0 (C-3', C-5'), 122.1 (C-2, C-6); EIMS  $m/z$  [M+H]<sup>+</sup> 216.05 (calcd. 215.05).

**(E)-1-[N-(4-fluorophenyl)]-1-phenylmethanimine (3f)**

A bright white solid was obtained in 50% yield; 54-56 °C;  $R_f$  0.90 (*n*-hexane/AcOEt 7:3); UV-Vis (MeOH):  $\lambda_{\max}$  = 266.2  $\pm$  1.6 nm,  $\epsilon$  = 150470 mol<sup>-1</sup>·dm<sup>3</sup>·cm<sup>-1</sup>; IR = 1570.88 (-C=N-), 1619.96, 1485.01, 1448.20 (aromatic), 753.00 (-C-F), 830.70 (*para*-substituted) cm<sup>-1</sup>; <sup>1</sup>H NMR (CDCl<sub>3</sub>, 600 MHz):  $\delta$  = 8.53 (-HC=N-, 1H, s), 8.00-7.98 (H2', H6', 2H, m), 7.56-7.55 (H3', H4', H5', 3H, m), 7.30 (H2, H6, 2H, d, <sup>3</sup>J<sub>H-H</sub> = 7.0 Hz), 7.47 (H3, H5, 2H, d, <sup>3</sup>J<sub>H-H</sub> = 7.0 Hz); <sup>13</sup>C NMR (CDCl<sub>3</sub>, 150 MHz):  $\delta$  = 160.4 (-HC=N-), 152.1 (C-1), 136.2 (C-1'), 131.4 (C-4'), 129.1 (C-2', C-6'), 128.80 (C-3', C-5'), 128.85 (C-2, C-6), 125.9 (C-4), 120.9 (C-3, C-5); EIMS  $m/z$  [M+H]<sup>+</sup> 200.08 (calcd. 199.22).

**(E)-1-[N-(4-methoxyphenyl)]-1-phenylmethanimine (3g)**

A bright grey solid was provided in 75% yield; 70–72 °C;  $R_f$  0.76 (*n*-hexane/AcOEt 7:3); UV-Vis (MeOH):  $\lambda_{\max} = 285.3 \pm 49.75$  nm,  $\epsilon = 132680$  mol<sup>-1</sup>·dm<sup>3</sup>·cm<sup>-1</sup>; IR = 2953.11 (CH<sub>3</sub>, -CH<sub>2</sub>-), 1574.97 (-C=N-), 1497.27 (aromatic), 1104.69 (-C-O-CH<sub>3</sub>), 834.79 (*para*-substituted) cm<sup>-1</sup>; <sup>1</sup>H NMR (CDCl<sub>3</sub>, 600 MHz):  $\delta$  = 8.55 (-HC=N-, 1H, s), 7.97–7.96 (H2', H6', 2H, m), 7.53–7.53 (H3', H4', H5', 3H, m), 7.32 (H2, H6, 2H, d, <sup>3</sup>*J*<sub>H-H</sub> = 9.0 Hz), 7.01 (H3, H5, 2H, d, <sup>3</sup>*J*<sub>H-H</sub> = 8.4 Hz), 3.89 (-CH<sub>3</sub>, 3H, s); <sup>13</sup>C NMR (CDCl<sub>3</sub>, 150 MHz):  $\delta$  = 158.3 (-HC=N-), 144.9 (C-1), 136.4 (C-1'), 131.1 (C-4'), 128.7 (C-2', C-6'), 128.6 (C-3', C-5'), 122.3 (C-2, C-6), 116.4 (C-4), 114.4 (C-3, C-5), 55.5 (-OCH<sub>3</sub>); EIMS *m/z* [M+H]<sup>+</sup> 212.10 (calcd. 211.10).

**Single-crystal X-ray crystallography**

Recrystallization of *N*-arylbenzylimine **3f** from CH<sub>2</sub>Cl<sub>2</sub>/*n*-hexane led to the formation of colorless crystals, one of which was mounted on a glass fiber. Crystallographic measurements were carried out at room temperature on an Oxford Diffraction Xcalibur S diffractometer with Mo K $\alpha$  radiation (graphite monochromator,  $\lambda_{\max} = 0.71073$  Å) and a CCD detector. Empirical absorption corrections were applied. The structure was solved with SHELXT and refined with SHELXL [36], both running within the WinGX environment [37]. Anisotropic temperature factors were introduced for all non-hydrogen atoms. Hydrogen atoms were placed in idealized positions, and their atomic coordinates refined by using unit weights. The plot in **Fig. 2** was made with PLATON [38, 39]. Data for *N*-arylbenzylimine **3f** are summarized in **Table 1**. Supplementary crystallographic data have been deposited at the Cambridge Crystallographic Data Centre (CCDC 2046921) [40].

**Table 1.** Crystallographic data of *N*-arylbenzylimine **3f**.

|  |   |
|--|---|
| Empirical formula  | C <sub>13</sub> H <sub>10</sub> FN  |
| Molecular weight   | 199.22  |
| Crystal size (mm)  | 0.49×0.26×0.16  |
| Crystal system   | Monoclinic  |
| Space group  | <i>P</i> 2 <sub>1</sub> / <i>n</i>  |
| Unit cell parameters (Å, °)                                  | <i>a</i> = 5.7528(3), $\alpha$ = 90<br><i>b</i> = 25.1417(11), $\beta$ = 90.198(5)<br><i>c</i> = 7.2892(4), $\gamma$ = 90 |
| Volume (Å <sup>3</sup> )                                     | 1054.27(9)  |
| <i>Z</i>   | 4   |
| Density (calcd, Mg/m <sup>3</sup> )                          | 1.255   |
| Absorption coefficient ( $\mu$ , mm <sup>-1</sup> )          | 0.086   |
| $\theta$ range for data collection (°)                       | 3.231–32.461  |
| Reflections collected  | 6489  |
| Independent reflections                                      | 3203  |
| Observed reflections   | 1932  |
| Goodness-of-fit on F <sup>2</sup>                            | 1.028   |
| Final <i>R</i> indices [ <i>I</i> > 2 $\sigma$ ( <i>I</i> )] | <i>R</i> <sub>1</sub> = 0.0610, <i>wR</i> <sup>2</sup> = 0.1236   |

**General method for the preparation of the solutions: positive controls and (E) N-arylbenzylamines**

The solutions of the positive control were prepared by taking successive 1:10 aliquots from the stock solution (14.6743 mg aztreonam, 337  $\mu$ M) in order to construct the standard curve and calculate the MIC [41–43]. Successive solutions of the *N*-arylbenzylamines were prepared to obtain the gradual concentration-response curves and calculate the MIC values. From the stock solution (4.0 mM), the dilutions were elaborated at 400, 200, 175, 150, 125, 100, 75, and 50  $\mu$ M. The compounds were added according to the general method to furnish 4.0 mM, requiring 7.2496 mg of **3a**, 15.3565 mg of **3b**, 9.0100 mg of **3c**, 13.0065 mg of **3d**, 8.6272 mg of **3e**, 7.9692 mg of **3f** and 8.4504 mg of **3g**. Methanol served as the negative control [41–43].

The *N*-arylbenzylamines derivatives showed stability under the conditions in which the experiments were conducted. The stock solutions did not show any change during preparation, whether in appearance, coloration, or the formation of precipitates. They remained translucent, which allowed for the preparation of successive dilutions with the same characteristics.

### ***In vitro* antibacterial activity**

#### **Bacterial strains**

All the materials used for culturing the bacterium and conducting the *in vitro* microbiological assays were autoclaved at 121 °C and 15 psi for 20 min. Bacterial lyophilizate, taken from *P. aeruginosa* ATCC 27853, was activated in nutritive broth containing 1.0 L pancreatic digest comprised of 5.0 g gelatin and 3.0 g of an extract of bovine meat (at pH 7.3 ± 0.2). It was seeded by cross striation in the culture medium of trypticase soy agar (TSA) containing 1.0 L pancreatic digest constituted by 15.0 g casein and papaic digest of 5.0 g soy flour, 5.0 g NaCl and 15.0 g agar (at pH 7.3 ± 0.2). Primary biochemical evaluations (the gram stain, oxidase and catalase tests) were employed to assure the purity of the strains and confirm their identity [44].

#### **Quantitative assessment of biological activity**

Antibacterial activity was examined *in vitro* by the agar diffusion method (Kirby-Bauer). Live cells of *P. aeruginosa* were harvested from the TSA medium at 18-24 h of growth. They were suspended in 0.85% (m/V) saline with a density of 1.5x10<sup>6</sup> colony forming units (CFU)/mL (0.5 McFarland units), measured at an absorbance of 625 nm in a range of 0.08-0.10 AU on a Model CS-200 PC Globe spectrophotometer and a Model Vortex-Mixer Fisher Scientific shaker. Subsequently, this suspension (1.5x10<sup>6</sup> CFU/mL) was seeded with sterile swabs in the Müeller-Hinton agar culture medium, which was composed of 2.0 g beef extract, 17.5 g hydrolyzed casein acid, 1.5 g starch and 17.0 g agar (at pH 7.3 ± 0.2).

After placing 6 Sensi discs in each Petri dish, 10 µL of one of the compounds was added (positive control, negative control, and 50, 75, 100, 125, 150, 175, 200, and 400 µM of the corresponding *N*-arylbenzylamine). The plates were inverted and incubated for 24 h at 37 °C, and then the inhibition halos were measured with a Vernier [41-43]. The MICs were determined for the reference and test compounds [45-47]. The aztreonam-induced inhibition was taken as 100%, and the inhibitory activity of the test compounds was expressed as a relative percentage. Each *N*-arylbenzylamine was examined by constructing a gradual concentration-response curve. MIC values, calculated by the Hill method, were considered equivalent to the CE<sub>95</sub> value [48], according to the following equation:

$$\log\left(\frac{E_0}{E_{\max}-E_0}\right) = n_H \log C - n_H \log CE_{95}$$

#### **QSAR study**

The QSAR was performed under QSAR-2D, proposed by Corwin Hansch and Toshio Fujita [49, 50]. Concerning the physicochemical properties of the *N*-arylbenzylamines, size was measured by molar refractivity (Advanced Chemistry Development, Inc.) and lipophilicity by the partition coefficient [51, 52]. These parameters were determined on ACD/ChemSketch 2015 and CS ChemDraw Pro v.6 software, respectively [53].

The lipid solubility descriptor was established by the following equation:

$$\pi = \log\left(\frac{P_X}{P_H}\right)$$

where,  $\pi$  is the lipid solubility descriptor, and  $P_X$  and  $P_H$  are the partition coefficients of a given substituted compound and the reference drug, respectively.

The Hammett *para* substituent constant ( $\sigma_p$ ) was utilized as the criterion of electronic effects [54, 55]. The steric descriptor was calculated by means of the following equation:

$$E_s = \log \left( \frac{MR_X}{MR_H} \right)$$

Where  $E_s$  is the steric descriptor proposed by Taft [56, 57], and  $MR_x$  and  $MR_H$  are the molar refractivity of a given substituted compound and the reference drug, respectively.

### Statistical analysis

Data were examined by using simple linear regression analysis with the least-squares technique and one-way ANOVA. The slopes were ordered to the origin and linear correlation coefficients were compared to the controls by the Student's  $t$ -test. Significance was considered at  $p < 0.05$  in all cases. The QSAR model was analyzed by utilizing multiple regression analysis with the determinant technique and one-way ANOVA. Statistical evaluations were run on Sigma Stat 4.0 (Systat Software Inc., San Jose, CA, USA). The external prediction of the QSAR models was assessed by the predictive squared correlation coefficient ( $Q^2$ ) [58], calculated by the following equation:

$$Q^2 = 1 - \frac{\sum_{i=0}^n (\overline{MIC}_{calc} - MIC_{expi})^2}{\sum_{i=0}^n (MIC_{expi} - \overline{MIC}_{exp})^2} = 1 - \frac{PRESS}{SS}$$

Where  $PRESS$  is the index related to the predictive residual sum of squares, and  $SS$  is the activity sum of squares.

## Results and discussion

### *In silico* study

#### Determination of the ADMET properties

The physicochemical characteristics of the seven *N*-arylbenzylimines (**3a-g**) are described by their ADMET properties (**Table 2**).

**Absorption:** The degree of fat solubility of the *N*-arylbenzylimines allows them to cross intestinal cell membranes and therefore reach sufficient concentrations in the central compartment. On the other hand, these compounds do not undergo any change in their structure at pH values greater than 4.5, and therefore could be highly absorbable in the duodenum. The exception is compound **3c** (-COOH), which would have a lower absorption rate because of being a conjugate base.

**Distribution:** Once the compounds reach the general circulation, they have a probability of binding to plasma proteins in the range of 43.0-74.0%. The lowest binding percentage is for **3a** (-H) and the highest for **3e** (-Cl). Thus, the free fraction of the *N*-arylbenzylimines should be adequately distributed in the body, since they have high enough log P values to be able to cross the cell membranes of some organs and tissues, such as the blood-brain barrier (BBB).

**Metabolism:** *N*-arylbenzylimines are susceptible to metabolic biotransformation by CYP450. Considering the oral route (the most common route of administration), these compounds undergo adequate absorption. However, they are susceptible to the first-pass effect, since their oral bioavailability ( $F_{oral}$ ) ranges from 0.50-0.66.

Overall, the *N*-arylbenzylimines show a greater tendency to inhibit the CYP isoforms 3A4, 2C9 and 2D6 than act as substrates of the same. The inhibition of CYP450 enzymes is important from the clinical point of view, because they represent a potential risk of drug-drug interactions, which occurs for example with some groups of antibiotics such as macrolides, fluoroquinolones and antiamebic agents from the group of metronidazole [59].

In case *N*-arylbenzylimines are capable of acting as a substrate for CYP450, there is the potential risk of drug-drug interactions, as well as the formation of inactive, active and/or toxic metabolites. The greatest probability of biotransformation reactions mediated by CYP3A4 and CYP2D6 are aromatic hydroxylation and *O*-dealkylation. The former could possibly involve all derivatives (**3a-g**), while the latter would apply only to

**3g (Table 3).** The greatest activity of the CYP3A4 isoform is on the disubstituted ring and the imine nitrogen, while that of the CYP2D6 isoform is the oxidation of the monosubstituted aromatic ring (**Table 3**).

*Elimination:* The oxidation of *N*-arylbenzylimines by CYP450 generates more polar molecules, which would mainly lead to their renal excretion due to their high water solubility and low molecular weight ( $M < 500$  g/mol).

**Table 2.** Physicochemical properties of the *N*-arylbenzylimines.

| Physicochemical properties                           | Compound |         |            |          |          |         |                         |
|--|----------|---------|------------|----------|----------|---------|-------------------------|
|  | 3a (-H)  | 3b (-I) | 3c (-COOH) | 3d (-Br) | 3e (-Cl) | 3f (-F) | 3g (-OCH <sub>3</sub> ) |
| Molecular weight g/mol                               | 181.09   | 306.99  | 225.08     | 259.00   | 215.05   | 199.22  | 211.10                  |
| Num. heavy atoms                                     | 14       | 15      | 17         | 15       | 15       | 15      | 16                      |
| Num. aromatic heavy atoms                            | 12       | 12      | 12         | 12       | 12       | 12      | 12                      |
| Fraction $C_{sp^3}$                                  | 0.00     | 0.00    | 0.00       | 0.00     | 0.00     | 0.00    | 0.07                    |
| Num. rotatable bonds                                 | 2        | 2       | 3          | 2        | 2        | 2       | 3                       |
| Num. H-bond acceptors                                | 1        | 1       | 3          | 1        | 1        | 2       | 2                       |
| Num. H-bond donors                                   | 0        | 0       | 1          | 0        | 0        | 0       | 0                       |
| Molar Refractivity                                   | 60.14    | 72.86   | 67.10      | 67.84    | 65.15    | 60.10   | 66.63                   |
| TPSA Å <sup>2</sup>                                  | 12.36    | 12.36   | 49.66      | 12.36    | 12.36    | 12.36   | 21.59                   |
| <b>Lipophilicity</b>                                 |          |         |            |          |          |         |                         |
| Log $P_{o/w}$ (iLOGP)                                | 2.50     | 2.86    | 2.06       | 2.90     | 2.77     | 2.63    | 2.81                    |
| Log $P_{o/w}$ (XLOGP3)                               | 2.82     | 3.47    | 2.35       | 3.51     | 3.45     | 2.92    | 2.79                    |
| Log $P_{o/w}$ (WLOGP)                                | 3.44     | 4.04    | 3.14       | 4.20     | 4.09     | 4.00    | 3.45                    |
| Log $P_{o/w}$ (MLOGP)                                | 3.26     | 4.05    | 2.72       | 3.93     | 3.80     | 3.67    | 2.87                    |
| Log $P_{o/w}$ (SILICOS-IT)                           | 3.90     | 4.83    | 3.26       | 4.54     | 4.50     | 4.28    | 3.88                    |
| Consensus Log $P_{o/w}$                              | 3.18     | 3.85    | 2.70       | 3.81     | 3.72     | 3.50    | 3.16                    |
| <b>ADMET predicted profile</b>                       |          |         |            |          |          |         |                         |
| <b>A (Absorption)</b>                                |          |         |            |          |          |         |                         |
| Blood-brain barrier (BBB) penetration                | 0.9962   | 0.9926  | 0.9434     | 0.9926   | 0.9911   | 0.9918  | 0.9775                  |
| Human intestinal absorption (HIA)                    | 0.9730   | 0.9319  | 0.9474     | 0.9649   | 0.9749   | 0.9734  | 0.9825                  |
| Human oral bioavailability (HOB)                     | 0.5857   | 0.5000  | 0.6571     | 0.5429   | 0.5857   | 0.5714  | 0.5000                  |
| Caco-2-permeability                                  | 0.9070   | 0.8085  | 0.8062     | 0.8494   | 0.8565   | 0.9207  | 0.9367                  |
| P-glycoprotein inhibitor                             | 0.9815   | 0.9774  | 0.9646     | 0.9670   | 0.9682   | 0.9692  | 0.9365                  |
| P-glycoprotein substrate                             | 0.9879   | 0.9761  | 0.9822     | 0.9840   | 0.9899   | 0.9560  | 0.9695                  |
| <b>D (Distribution)</b>                              |          |         |            |          |          |         |                         |
| Subcellular location: Mitochondria                   | 0.4784   | 0.5888  | 0.6476     | 0.5111   | 0.5950   | 0.6152  | 0.6539                  |
| <b>M (Metabolism)</b>                                |          |         |            |          |          |         |                         |
| <b>Cytochrome P450 (CYP450) substrate, inhibitor</b> |          |         |            |          |          |         |                         |
| CYP3A4 substrate                                     | 0.8087   | 0.7411  | 0.7660     | 0.7322   | 0.6478   | 0.7202  | 0.6432                  |
| CYP2C9 substrate                                     | 0.5856   | 0.5878  | 0.8032     | 0.5878   | 0.6261   | 0.6017  | 0.5878                  |
| CYP2D6 substrate                                     | 0.7217   | 0.7395  | 0.8785     | 0.7383   | 0.7585   | 0.7344  | 0.6843                  |



|  |        |        |        |        |        |        |        |
|--|--------|--------|--------|--------|--------|--------|--------|
| CYP3A4 inhibitor                                   | 0.9568 | 0.9372 | 0.9578 | 0.9518 | 0.9392 | 0.9443 | 0.7476 |
| CYP2C9 inhibitor                                   | 0.9269 | 0.9077 | 0.9252 | 0.8505 | 0.9106 | 0.9100 | 0.8828 |
| CYP2C19 inhibitor                                  | 0.6873 | 0.7239 | 0.8843 | 0.7872 | 0.8198 | 0.6449 | 0.5612 |
| CYP2D6 inhibitor                                   | 0.6535 | 0.5092 | 0.8502 | 0.6208 | 0.6064 | 0.6950 | 0.8435 |
| CYP1A2 inhibitor                                   | 0.7705 | 0.9484 | 0.6455 | 0.9158 | 0.9414 | 0.9047 | 0.8552 |
| CYP inhibitory promiscuity                         | 0.6829 | 0.6997 | 0.9130 | 0.7371 | 0.7180 | 0.6651 | 0.7467 |
| <b>Drug transporters in pharmacokinetics</b>       |        |        |        |        |        |        |        |
| OATP2B1 inhibitor                                  | 1.0000 | 1.0000 | 1.0000 | 1.0000 | 1.0000 | 1.0000 | 1.0000 |
| OATP1B1 inhibitor                                  | 0.9430 | 0.9016 | 0.9297 | 0.9038 | 0.9082 | 0.9274 | 0.9040 |
| OATP1B3 inhibitor                                  | 0.9528 | 0.9509 | 0.9464 | 0.9508 | 0.9516 | 0.9519 | 0.9631 |
| MATE1 inhibitor                                    | 1.0000 | 1.0000 | 0.9800 | 1.0000 | 0.9000 | 1.0000 | 0.9600 |
| OCT2 inhibitor                                     | 0.7500 | 0.7750 | 0.9750 | 0.7750 | 0.8000 | 0.7750 | 0.7250 |
| BSEP inhibitor                                     | 0.5759 | 0.6161 | 0.6979 | 0.6664 | 0.5721 | 0.5120 | 0.6124 |
| <b>T (Toxicity)</b>                                |        |        |        |        |        |        |        |
| <b>Organ toxicity</b>                              |        |        |        |        |        |        |        |
| Hepatotoxicity                                     | 0.6250 | 0.5250 | 0.7500 | 0.5750 | 0.6000 | 0.5750 | 0.6500 |
| Human ether-a-go-go-related gene (hERG) inhibition | 0.5723 | 0.6390 | 0.7617 | 0.5099 | 0.4685 | 0.4220 | 0.6873 |
| Eye corrosion                                      | 0.9123 | 0.8324 | 0.9298 | 0.9387 | 0.9418 | 0.9294 | 0.9119 |
| Eye irritation                                     | 0.9966 | 0.8651 | 0.9599 | 0.9503 | 0.9048 | 0.9069 | 0.9702 |
| Estrogen receptor binding                          | 0.8236 | 0.9015 | 0.9394 | 0.9052 | 0.9160 | 0.8763 | 0.8815 |
| Androgen receptor binding                          | 0.8062 | 0.6558 | 0.5248 | 0.4929 | 0.5591 | 0.6429 | 0.7434 |
| Thyroid receptor binding                           | 0.5858 | 0.5349 | 0.6916 | 0.5143 | 0.5160 | 0.5627 | 0.5395 |
| Glucocorticoid receptor binding                    | 0.6120 | 0.4737 | 0.6554 | 0.6016 | 0.5485 | 0.5523 | 0.5807 |
| Aromatase binding                                  | 0.8636 | 0.8324 | 0.8750 | 0.8454 | 0.8233 | 0.7086 | 0.7297 |
| PPAR $\gamma$                                      | 0.8093 | 0.7090 | 0.7858 | 0.9066 | 0.8889 | 0.7891 | 0.5638 |
| <b>Toxicogenomics</b>                              |        |        |        |        |        |        |        |
| Ames mutagenicity                                  | 0.7100 | 0.6600 | 0.5400 | 0.6200 | 0.5300 | 0.7300 | 0.6500 |
| Carcinogenicity (binary)                           | 0.5336 | 0.5336 | 0.6626 | 0.5194 | 0.5479 | 0.5336 | 0.6075 |
| Carcinogenicity (ternary)                          | 0.5455 | 0.6711 | 0.6198 | 0.5808 | 0.6727 | 0.6390 | 0.5216 |
| Micronuclear                                       | 0.7299 | 0.7032 | 0.6900 | 0.7032 | 0.7632 | 0.6332 | 0.5600 |
| <b>Eco-toxicity</b>                                |        |        |        |        |        |        |        |
| Biodegradation                                     | 0.9250 | 0.9500 | 0.8000 | 0.9250 | 0.9500 | 0.9500 | 0.9500 |
| Honey bee toxicity                                 | 0.6907 | 0.6535 | 0.7249 | 0.6372 | 0.6509 | 0.6431 | 0.5000 |
| Aquatic toxicity (crustaceans)                     | 0.8600 | 0.8800 | 0.7100 | 0.8700 | 0.9200 | 0.8600 | 0.9100 |
| Aquatic toxicity (fish)                            | 0.9489 | 0.9877 | 0.9416 | 0.9890 | 0.9876 | 0.9878 | 0.8363 |
| <b>ADMET predicted profile-Regressions</b>         |        |        |        |        |        |        |        |
| Water solubility (logS)                            | -3.803 | -4.633 | -3.153 | -4.515 | -4.471 | -3.657 | -3.889 |
| Plasma protein binding                             | 0.439  | 0.731  | 0.680  | 0.650  | 0.732  | 0.583  | 0.554  |

|  |       |       |       |       |       |       |       |
|--|-------|-------|-------|-------|-------|-------|-------|
| Acute oral toxicity<br>(mol/kg)                        | 1.914 | 1.866 | 1.866 | 2.187 | 2.088 | 2.123 | 1.729 |
| Tetrahymena<br>pyriformis pIGC <sub>50</sub><br>(µg/L) | 0.559 | 1.826 | 0.496 | 1.875 | 1.684 | 1.322 | 1.144 |

According to the results of the *in silico* study, the *N*-arylbenzylamines do not violate any of the acceptability standards of Lipinski's rule of five. Their fat solubility, size and polarity values indicate a capacity to easily cross cell membranes, such as the BBB and enterocytes, allowing them to reach plasma concentrations adequate for producing the desired pharmacological effect. The antibacterial activity found for the present *N*-arylbenzylamines is in agreement with their adsorption properties. The biological membranes they can cross include those of Gram-negative bacteria.

**Table 3.** Predicted site of metabolism for cytochrome P450s.

| Compound                     | Structure | Atom | 3A4<br>Score | Energy<br>(kJ/mol) | Structure | Atom | 2D6<br>Score | Energy<br>(kJ/mol) |
|------------------------------|-----------|------|--------------|--------------------|-----------|------|--------------|--------------------|
| <b>3a (-H)</b>               |           | C.12 | 58.8         | 68.2               |           | C.12 | 66.8         | 68.2               |
|                              |           | C.10 | 69.7         | 77.2               |           | C.7  | 79.4         | 80.8               |
|                              |           | C.14 | 69.7         | 77.2               |           | C.10 | 89.3         | 77.2               |
|                              |           | N.2  | 70.6         | 75.6               |           | C.14 | 89.3         | 77.2               |
|                              |           | C.7  | 71.4         | 80.8               |           | C.6  | 91.6         | 86.3               |
| <b>3b (-I)</b>               |           | C.4  | 70.4         | 77.2               |           | C.11 | 79.4         | 80.8               |
|                              |           | N.6  | 71.0         | 75.6               |           | C.10 | 91.6         | 86.3               |
|                              |           | C.11 | 71.4         | 80.8               |           | C.9  | 93.0         | 80.8               |
|                              |           | C.9  | 73.2         | 80.8               |           | C.4  | 96.1         | 77.2               |
|                              |           | C.3  | 76.6         | 84.1               |           | C.3  | 96.4         | 84.1               |
| <b>3c (-COOH)</b>            |           | N.8  | 70.7         | 75.6               |           | C.13 | 79.4         | 80.8               |
|                              |           | C.6  | 71.0         | 77.2               |           | C.12 | 91.6         | 86.3               |
|                              |           | C.13 | 71.4         | 80.8               |           | C.11 | 93.0         | 80.8               |
|                              |           | C.11 | 73.0         | 80.8               |           | C.5  | 99.8         | 80.8               |
|                              |           | C.5  | 73.9         | 80.8               |           | N.8  | 1001.9       | 75.6               |
| <b>3d (-Br)</b>              |           | C.4  | 70.4         | 77.2               |           | C.11 | 79.4         | 80.8               |
|                              |           | N.6  | 71.0         | 75.6               |           | C.10 | 91.6         | 86.3               |
|                              |           | C.11 | 71.4         | 80.8               |           | C.9  | 93.0         | 80.8               |
|                              |           | C.9  | 73.2         | 80.8               |           | C.4  | 96.1         | 77.2               |
|                              |           | C.3  | 76.6         | 84.1               |           | C.3  | 96.4         | 84.1               |
| <b>3e (-Cl)</b>              |           | C.4  | 70.4         | 77.2               |           | C.11 | 79.4         | 80.8               |
|                              |           | N.6  | 71.0         | 75.6               |           | C.10 | 91.6         | 86.3               |
|                              |           | C.11 | 71.4         | 80.8               |           | C.9  | 93.0         | 80.8               |
|                              |           | C.9  | 73.2         | 80.8               |           | C.4  | 96.1         | 77.2               |
|                              |           | C.3  | 76.6         | 84.1               |           | C.3  | 96.3         | 84.1               |
| <b>3f (-F)</b>               |           | C.4  | 70.4         | 77.2               |           | C.11 | 79.4         | 80.8               |
|                              |           | N.6  | 71.0         | 75.6               |           | C.10 | 91.6         | 86.3               |
|                              |           | C.11 | 71.4         | 80.8               |           | C.9  | 93.0         | 80.8               |
|                              |           | C.9  | 73.2         | 80.8               |           | C.4  | 96.1         | 77.2               |
|                              |           | C.3  | 76.6         | 84.1               |           | C.3  | 96.3         | 84.1               |
| <b>3g (-OCH<sub>3</sub>)</b> |           | C.1  | 51.5         | 62.2               |           | C.1  | 59.5         | 62.2               |
|                              |           | C.4  | 70.2         | 77.2               |           | C.12 | 79.4         | 80.8               |
|                              |           | N.7  | 70.7         | 75.6               |           | C.11 | 91.6         | 86.3               |
|                              |           | C.5  | 71.0         | 77.2               |           | C.10 | 93.0         | 80.8               |
|                              |           | C.12 | 71.4         | 80.8               |           | C.4  | 96.1         | 77.2               |

**Toxicity:** In relation to the acute toxicity of *N*-arylbenzylimines **3a-g**, the LD<sub>50</sub> are greater than 5000 mg/kg, indicating safe substances. Regarding toxicogenomics, these compounds have moderate activity. However, the harmful effects would be caused by chronic exposure.

### Synthesis and characterization

Seven *para*-substituted *N*-arylbenzylimines were obtained in solid form with medium polarity and moderate to high yields ( $\geq 50\%$ ). As for the NMR determination of their relative configuration, the nuclear Overhauser effect (NOE) experiment conclusively demonstrated the *E*-configuration for all seven molecules. When the hydrogen corresponding to the formation of the *N*-arylbenzylimines was irradiated, **3b** was displaced at approximately 8.4 ppm (**Fig. 1**). The hydrogens that undergo this displacement are H2 and H6, giving signals at 6.9 and 7.0 ppm, respectively.

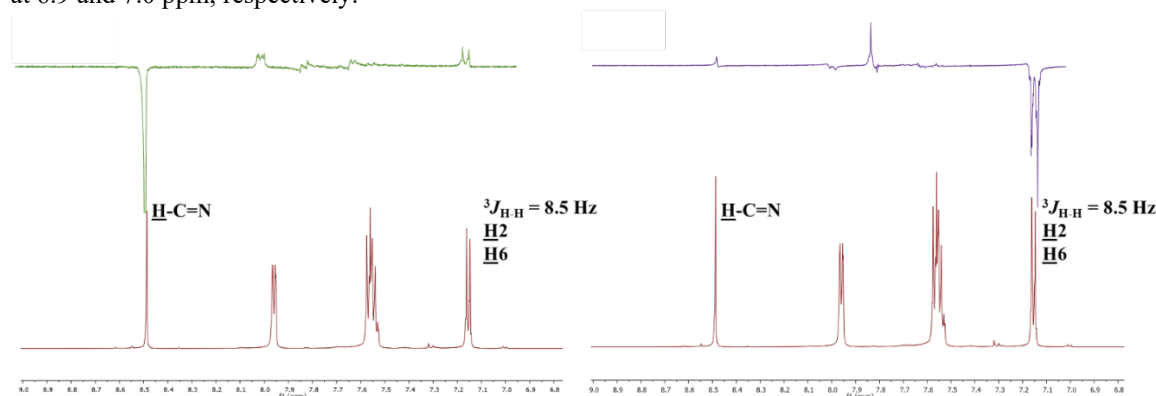


**Fig. 1.** NMR spectrum, revealing the NOE (600 MHz; CDCl<sub>3</sub>) of *N*-arylbenzylimine **3b** (-I).

After the selective irradiation of the imine hydrogen, there was a disturbance in the intensity of the signals of the H2 and H6 hydrogens, which indicates nuclear spin polarization transfer in the space between these hydrogens. Clearly, this could only occur for the *E*-configuration of the *N*-arylbenzylimines, which should be favored on the basis of the steric effects of the aromatic rings.

### Single-crystal X-ray crystallography

The *E*-configuration of *N*-arylbenzylimine **3f** was further supported by single-crystal X-ray diffraction analysis (**Fig. 2**).

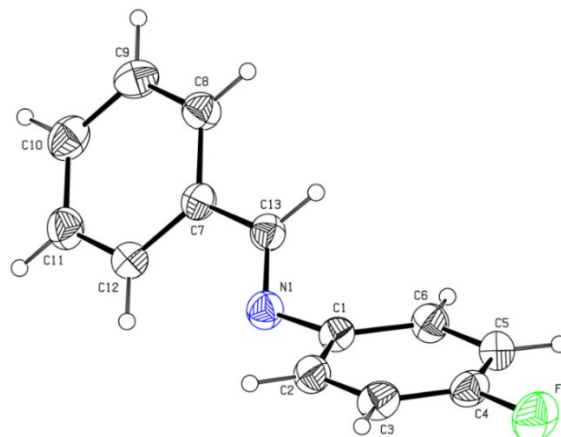
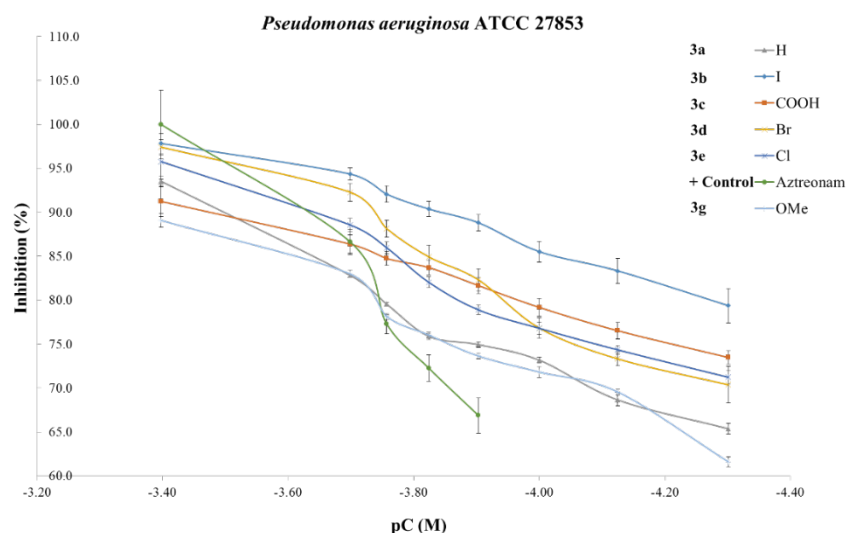


**Fig. 2.** Oak Ridge thermal ellipsoid plot (ORTEP) of the structure obtained by single-crystal X-ray diffraction of *N*-arylbenzylimine **3f**. The diagram was drawn with 30% thermal ellipsoid probability.

### *In vitro* antibacterial activity

Regarding macroscopic morphology, the cultured bacteria was seen in small colonies with irregular and translucent edges [60]. The microscopic morphology of the bacteria corresponds to isolated Gram-negative bacilli. The primary biochemical evaluations found were the following: Gram-, catalase+ and oxidase+ [61, 62].

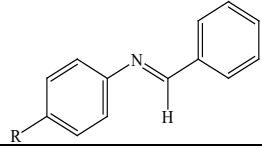
On the other hand, most of the compounds (**3a-e** and **g**) generated good inhibitory activity on *P. aeruginosa*, in the range of 90-95% (relative to aztreonam). Since all the relevant *N*-arylbenzylamines displayed similar slopes of the concentration-response curve, they likely have the same mechanism of action. Contrarily, the slope of aztreonam was different (**Fig. 3**).



**Fig. 3.** Concentration-response curves of the percentage of partial inhibition of *P. aeruginosa* ATCC 27853 by the *para*-substituted *N*-arylbenzylamines and the positive control, aztreonam, based on their pC (M) concentrations. The inhibition produced by aztreonam is considered 100%.

The activity of the test compounds on *P. aeruginosa* is shown by the MIC values (**Table 4**), which are lower for **3b-d** (198.47, 249.60 and 290.20  $\mu$ M, respectively) than aztreonam (337.39  $\mu$ M).

**Table 4.** The MIC values of the *para*-substituted *N*-arylbenzylamines evaluated on *P. aeruginosa*.

|  | MIC $\pm$ SEM ( $\mu$ M) against <i>P. aeruginosa</i> ATCC 27853 |
|---|--|
| <b>3a (-H)</b>  | 790.10 $\pm$ 0.008   |
| <b>3b (-I)</b>  | 198.47 $\pm$ 0.082   |
| <b>3c (-COOH)</b>   | 249.60 $\pm$ 0.072   |
| <b>3d (-Br)</b>   | 290.20 $\pm$ 0.069   |
| <b>3e (-Cl)</b>   | 417.55 $\pm$ 0.041   |
| <b>3f (-F)</b>  | ND   |
| <b>3g (-OCH<sub>3</sub>)</b>  | 381.05 $\pm$ 0.028   |
| <b>Aztreonam</b>  | 337.39 $\pm$ 0.041   |

ND: Not determined

*N*-arylbenzylamines with substituents generally produced a better effect than the lead compound with hydrogen (MIC = 790.10  $\mu$ M). The derivative bearing the -I substituent (**3b**) (MIC = 198.47  $\mu$ M) was the most active of the test compounds, giving another indication that the antibacterial mechanism of action of the *N*-arylbenzylamines is probably different from that of the monobactam control drug, known to inhibit penicillin-binding proteins [63-67]. On the other hand, the MIC value for *N*-arylbenzylamine with substituent -F (**3f**) could not be determined because activity was only observed at the highest levels (200 and 400  $\mu$ M) of the concentration range selected (50-400  $\mu$ M).

### QSAR/SAR analysis

The QSAR analysis was conducted on the six relevant *N*-arylbenzylamines (**3a-e** and **g**) evaluated *in vitro* against *P. aeruginosa*. Their inhibitory activity was examined with the Hansch-Fujita model, which considers lipid solubility as well as electronic and steric effects. The substituents in molecules with the greatest antibacterial activity are bulky, electron-withdrawing and highly polar. Size was the most significant descriptor, as evidenced by the coefficient of 7.326.

$$\log \left( \frac{1}{\text{MIC}} \right) = -0.0589\pi * + 0.264\sigma * + 7.326E_s * + 3.111$$

$$r = 0.998*; Q^2 = 0.9964; N = 6; p < 0.05$$

Where  $\pi$  corresponds to lipid solubility,  $\sigma$  to the electronic effects in the *para* position, and  $E_s$  to the steric effects. The model provided adequate predictability and a good correlation value on *P. aeruginosa*. The calculated slope is very close to 1.0, and the linear correlation coefficient is  $r = 0.998$  (Fig. 4).

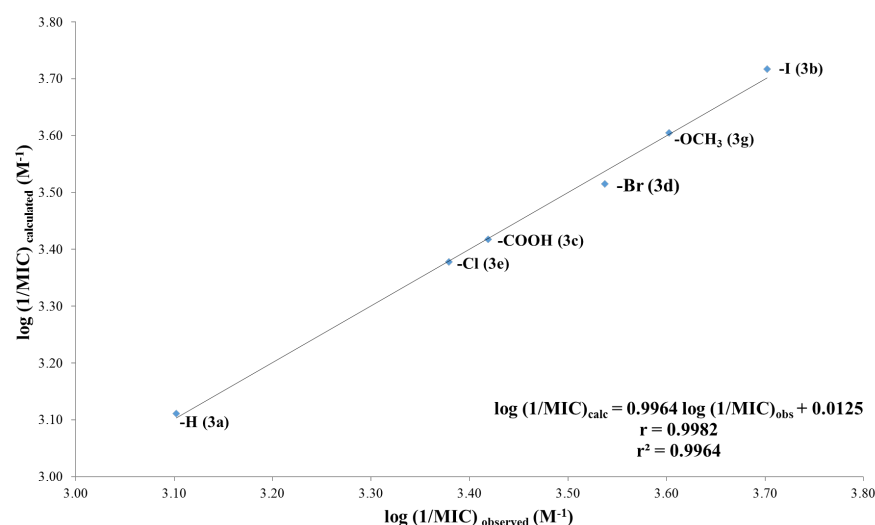


**Fig. 4.** The structure-activity relationship between the calculated log (1/MIC) ( $M^{-1}$ ) and observed log (1/MIC) ( $M^{-1}$ ) values of the six relevant *N*-arylbenzylamines tested on *Pseudomonas aeruginosa*. Simple linear regression analysis was performed with the least-squares technique, one-way ANOVA and ordinate values. The significance of the slope was determined by the Student's *t*-test:  $b = 0.012 \pm 0.104$  ( $*p < 0.05$ ),  $m = 0.996 \pm 0.030$  ( $*p < 0.001$ ) and  $r = 0.998$  ( $*p < 0.001$ ). Significance was considered at  $p < 0.05$ , with a 95.0% confidence level.

The *in vitro* experiment with **3f** afforded inhibition halos at concentrations of 200  $\mu$ M and 400  $\mu$ M. The size of the halos evidenced concentration dependence and suggested that the MIC value is probably greater than 400  $\mu$ M. Interestingly, the general QSAR model predicts a MIC of 724.56  $\mu$ M for **3f**, a value in accordance with the present results.

For the SAR analysis, the compounds were subclassified into G1 with resonance effects and G2 with inductive effects, taking **3a** as the point of reference. The values of the lipid solubility descriptor ( $\pi$ ) for the compounds in G1 (**3c** and **3g**) exhibited an inverse correlation with biological activity (the more polar substituents gave better antibacterial activity). For the compounds in G2 (**3b**, **3d** and **3e**), contrarily, a lower polarity of the substituent is associated with greater activity, resulting in a positive slope of the concentration-response curve (Fig. 5). Since **3f** bears a fluorine atom with inductive effects (similar to the other halogens), it would definitely fit into the G2 group.

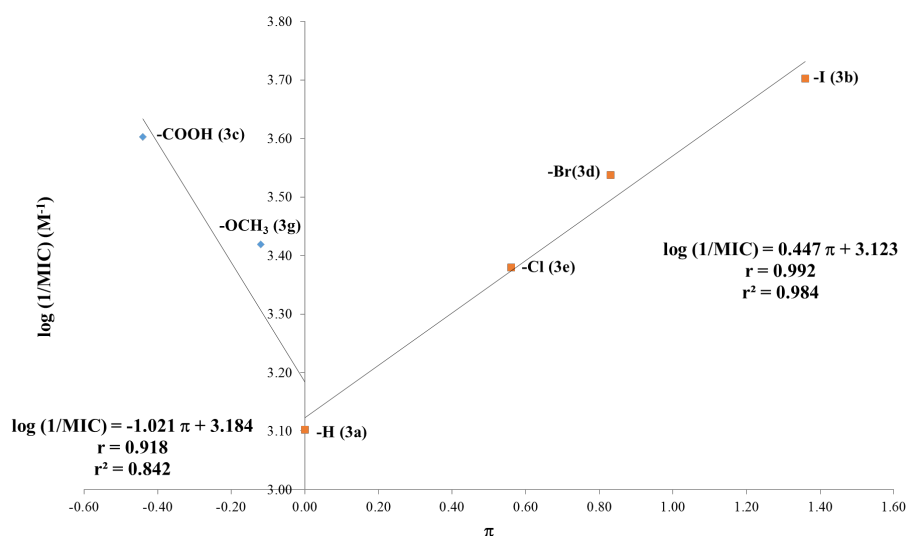


**Fig. 5.** The structure-activity relationship between the  $\log(1/\text{MIC})$  and  $\pi$ -values (the lipid solubility descriptor) of the six *N*-arylbenzylimines tested on *Pseudomonas aeruginosa*. Simple linear regression analysis was carried out with the least-squares technique, one-way ANOVA and ordinate values. The significance of the slope was determined by the Student's *t*-test. For G1:  $b = 3.184 \pm 0.116$  ( $*p < 0.023$ ),  $m = -1.021 \pm 0.442$  ( $*p = 0.260$ ) and  $r = 0.918$  ( $*p = 0.260$ ). For G2:  $b = 3.123 \pm 0.034$  ( $*p < 0.001$ ),  $m = 0.447 \pm 0.040$  ( $*p < 0.008$ ) and  $r = 0.992$  ( $*p < 0.008$ ). Significance was considered at  $p < 0.05$ , with a 95.0% confidence level.

Regarding the descriptor of electronic effects, both the G1 and G2 sets showed a linear correlation with a positive slope. In other words, the electron-withdrawing substituents of *N*-arylbenzylimines conferred greater antibacterial activity, with  $\rho$  values of 0.345 and 1.900, respectively. The difference in the magnitude of  $\rho$  evidences the sensitivity of the biological response to electronic effects. Better antibacterial activity was found for the inductive effects conferred by the halogens in G2 (**3b**, **3d** and **3e**) than the resonance effects of the other compounds in G1 (**3c** and **3g**) (Fig. 6). The inductive effects of **3f** would make it a halogenated compound belonging to the G2 group, though with the least antibacterial activity ( $\text{MIC} > 400 \mu\text{M}$ ) of the molecules in this group.

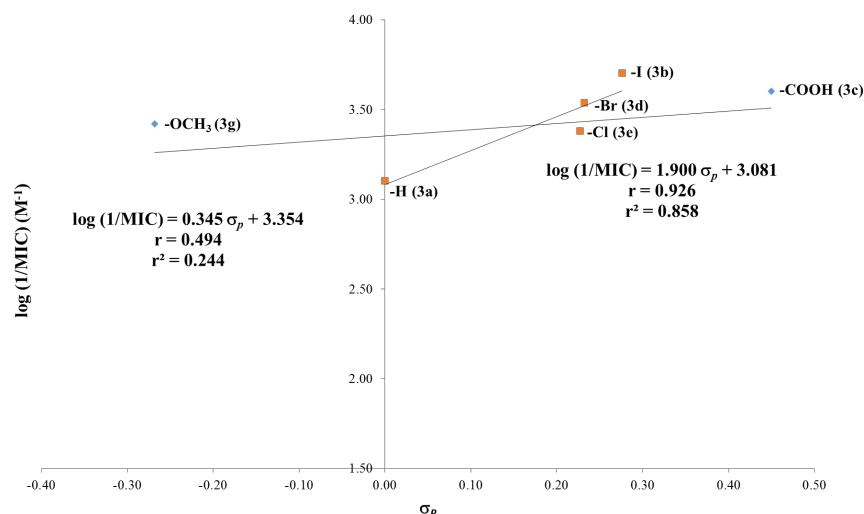


**Fig. 6.** The structure-activity relationship between the  $\log(1/\text{MIC})$  and  $\sigma_p$  values (the Hammett constant as the criterion of electronic effects) of the *N*-arylbenzylimines tested on *Pseudomonas aeruginosa*. Simple linear regression analysis was performed with the least-squares technique, one-way ANOVA and ordinate values. The significance of the slope was determined by the Student's *t*-test. For G1:  $b = 3.081 \pm 0.116$  ( $*p < 0.001$ ),  $m = 1.900 \pm 0.547$  ( $*p < 0.050$ ) and  $r = 0.926$  ( $*p < 0.050$ ). For G2:  $b = 3.354 \pm 0.183$  ( $*p < 0.035$ ),  $m = 0.345 \pm 0.607$  ( $*p = 0.671$ ) and  $r = 0.494$  ( $*p = 0.671$ ). Significance was considered at  $p < 0.05$ , with a 95.0% confidence level.

Concerning the steric descriptor ( $E_s$ ), antibacterial activity was correlated with the size of the molecule for both G1 and G2. The data plotted for each group forms a straight line with a positive slope. Hence, the biological effect increased with the size of the molecule, and molecular size was dependent on the substituent. The slope was very similar for the G1 and G2 sets (8.1423 and 7.2107, respectively), indicating the great susceptibility of biological activity to steric effects (**Fig. 7**). The molecules with the smallest substituents were **3a** (the lead compound) with a hydrogen atom and **3f** with a fluorine atom, which coincides with their relatively low biological activity.

The following interpretation is provided for how the *N*-arylbenzylimines crossed the bacterial barriers of *P. aeruginosa*. For G1, better activity was found for the highly polar compounds, **3c** and **3g** (especially the former). The  $-\text{COOH}$  substituent in compound **3c** generates a partial positive charge on the ring that delocalizes the positive charge ( $\rho = 0.345$ ), causing it to be repelled due to the positive charge on the outside of the outer membrane. Therefore, the molecule requires a transporter or a porin of the bacterium to pass through the membrane into the periplasmic space, where it strongly interacts with acidic peptidoglycan. For the G2 set (**3b**, **3d**, **3e** and **3f**), antibacterial activity was favored by high lipid solubility, suggesting the penetration of the external, cytoplasmic and cell wall membranes by simple diffusion. The polarizability and the soft base properties of the halogens give better interaction and affinity with the phospholipids of the membranes and with the peptidoglycan layer, thus explaining why they can cross by simple diffusion (**Fig. 8**). Rather than delocalizing any type of charge, these compounds have inductive electron-withdrawing effects.

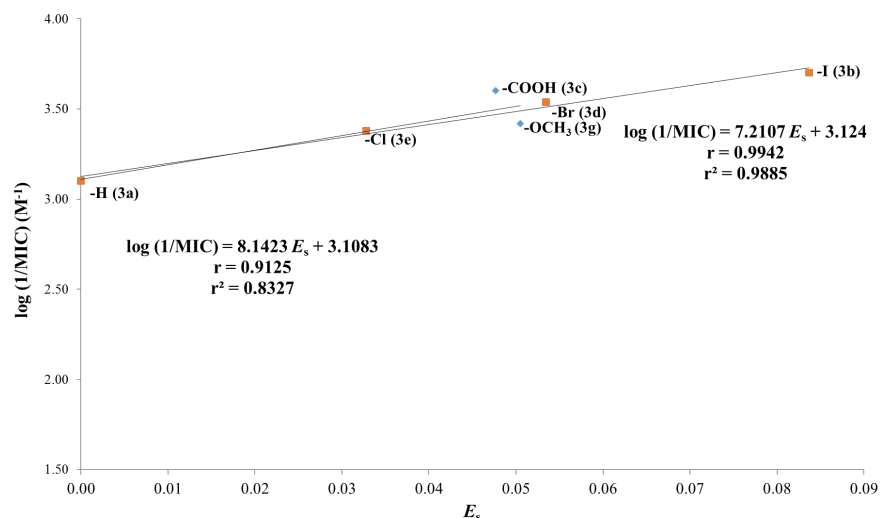


**Fig. 7.** The structure-activity relationship between  $\log(1/\text{MIC})$  and  $E_s$  (the steric descriptor) values of the six relevant *N*-arylbenzylimines tested on *Pseudomonas aeruginosa*. Simple linear regression analysis was carried out with the least-squares technique, one-way ANOVA and ordinate values. The significance of the slope was determined by the Student's *t*-test. For G1:  $b = 3.108 \pm 0.146$  ( $*p = 0.030$ ),  $m = 8.142 \pm 3.644$  ( $*p = 0.268$ ) and  $r = 0.913$  ( $*p = 0.268$ ). For G2:  $b = 3.124 \pm 0.113$  ( $*p = 0.033$ ),  $m = 7.2107 \pm 0.208$  ( $*p = 0.272$ ) and  $r = 0.994$  ( $*p = 0.302$ ). Significance was considered at  $p < 0.05$ , with a 95.0% confidence level.

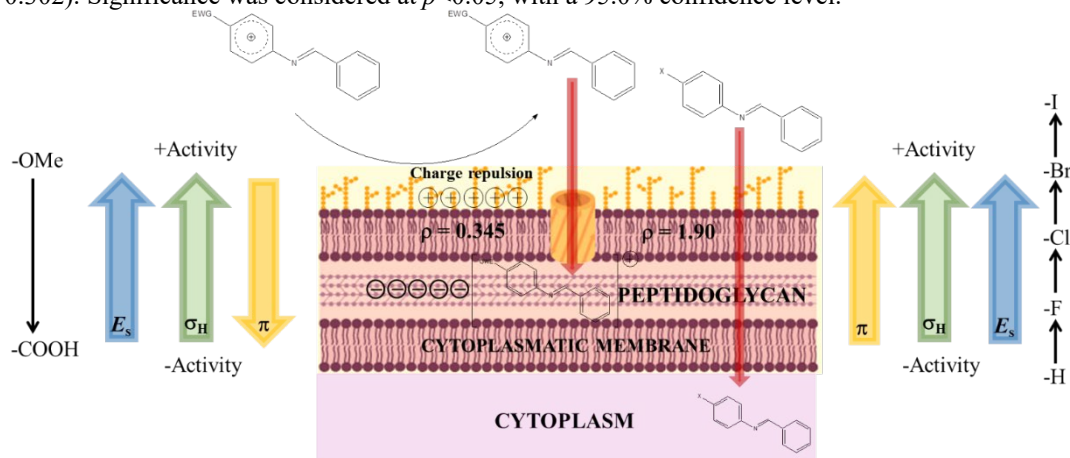


**Fig. 8.** Model illustrating the crossing of the membrane barriers of *Pseudomonas aeruginosa* by *N*-arylbenzylimines, based on the QSAR analysis.

## Conclusion

Seven *N*-arylbenzylimines were derived from *para*-substituted anilines and obtained in moderate to high yields with a simple synthetic methodology. They all showed an *E*-configuration, evidenced by NMR experiments and definitively confirmed by X-ray diffraction. These compounds displayed relevant inhibitory activity against *P. aeruginosa* compared to the corresponding reference drug, aztreonam. The microbiological data and the appraisal of the curves suggest that the mechanism of action is very likely the same for the seven *N*-arylbenzylimines, but different from that of the positive control. According to the QSAR analysis, biological activity is significantly dependent on steric effects, while lipid solubility and electronic effects play a vital role in the capacity of the molecules to cross the barriers of the bacterium. A greater capacity to penetrate these



barriers was found for the inductive effect of halogenated compounds than the resonance effect of the other compounds. The current physicochemical results are very important for the design and development of new molecules directed against multi-drug resistant *P. aeruginosa*, a highly infective and lethal pathogen.

## Acknowledgments

We are grateful to the Consejo Nacional de Ciencia y Tecnología (CONACyT, grant # 257364) and the SIP Project of the Instituto Politécnico Nacional (grants # 20181505 and 20196701) for providing the study with financial support.

JRMD is beholden to the Consejo Nacional de Ciencia y Tecnología (CONACyT, CVU # 889474) for the National Scholarship received and the program of the Beca de Estímulo Institucional de Formación de Investigadores (BEIFI, grant # 2018, registration 324 and 292, grant #2020, registration 260) for additional support. JAGS is a member of the EDI fellowship program of the IPN. JGTF and HAJV are members of the COFAA and EDI fellowship programs of the IPN. We thank Bruce Allan Larsen for proofreading the manuscript.

## References

1. Carreño, A.; Rodríguez, L.; Páez-Hernández, D.; Martín-Trasanco, R.; Zúñiga, C.; Oyarzún, DP.; Gacitúa, M.; Schott, E.; Arratia-Pérez, R.; Fuentes, JA. *Front. Chem.* **2018**, *6*, 1-13. DOI: <https://doi.org/10.3389/fchem.2018.00312>
2. Arunachalam, S.; Padma-Priya, N.; Jayabalakrishnan, C.; Chinnusamy, V. *Spectrochim. Acta A.* **2009**, *74*, 591-596. DOI: <https://doi.org/10.1016/j.saa.2009.06.061>
3. Chonan, Z-H.; Scozzafava, A.; Supuran, C-T. *J Enzyme Inhib. Med. Chem.* **2003**, *18*, 259-263. DOI: <https://doi.org/10.1080/1475636031000071817>
4. Guevara-Salazar, J-A.; Morán-Díaz, J-R.; Ramírez-Segura, E.; Trujillo-Ferrara, J-G. *Rev. Anti. Infect. Ther.* **2020**, 1-22. DOI: <https://doi.org/10.1080/14787210.2021.1839418>
5. Wise, R.; Hart, T.; Cars, O.; Streulens, M.; Helmuth, R.; Huovinen, P.; Sprenger, M. *BMJ.* **1998**, *317*, 609-610. DOI: <https://doi.org/10.1136/bmj.317.7159.609>
6. Beceiro, A.; Tomás, M.; Bou, G. *Clin. Microbiol. Rev.* **2013**, *26*, 185-230. DOI: <https://doi.org/10.1128/CMR.00059-12>
7. Shallcross, L.; Davies, D. *Br. J. Gen. Pract.* **2014**, *64*, 604-605. DOI: <https://doi.org/10.3399/bjgp14X682561>
8. Yelin, I.; Snitser, O.; Novich, G.; Katz, R.; Tal, O.; Parizade, M.; Chodick, G.; Koren, G.; Shalev, V.; Kishony, R. *Nat. Med.* **2019**, *25*, 1143-1152. DOI: <https://doi.org/10.1038/s41591-019-0503-6>
9. Aslam, B.; Wang, W.; Arshad, M.; Khurshid, M.; Muzammil, S.; Rasool, M.; Nisar, M.; Alvi, R.; Aslam, M.; Qamar, M.; Salamat, M.; Baloch, Z. *Infect. Drug. Resist.* **2018**, *10*, 1645-1658. DOI: <https://doi.org/10.2147/IDR.S173867>
10. Pang, Z.; Raudonis, R.; Glick, B.; Lin, T.; Cheng, Z. *Biotechnol. Adv.* **2018**, *37*, 177-192. DOI: <https://doi.org/10.1016/j.biotechadv.2018.11.013>
11. Colomb-Cotin, M.; Lacoste, J.; Brun-Buisson, C.; Jarlier, V.; Coignard, B.; Vaux, S. *Antimicrob. Resist. Infect. Control.* **2016**, *5*, 1-11. DOI: <https://doi.org/10.1186/s13756-016-0154-z>
12. Kobayashi, S.; Ishitani, H. *Chem. Rev.* **1999**, *99*, 1069-1094. DOI: <https://doi.org/10.1021/cr980414z>
13. Tietze, O.; Schiefner, B.; Ziemer, Z.; Zschunke, A. *Fresenius. J. Anal. Chem.* **1997**, *357*, 477-481. DOI: <https://doi.org/10.1007/s002160050195>

14. Bakkar, M.; Monshi, M.; Warad, I.; Siddiqui, M.; Bahajaj, A. *J. Saudi. Chem. Soc.* **2010**, *14*, 165-174. DOI: <https://doi.org/10.1016/j.jscs.2010.02.007>
15. Corre, Y.; Lali, W.; Hamdaoui, M.; Trivelli, X.; Djukic, J.P.; Agbossou-Niedercorn, F.; Michon, C. *Catal. Sci. Technol.* **2015**, *5*, 1452-1458. DOI: <https://doi.org/10.1039/C4CY01233J>
16. Franz, D.; Sirtl, L.; Pöthig, A.; Inoue, S. *Z. Anorg. Allg. Chem.* **2016**, *642*, 1245-1250. DOI: <https://doi.org/10.1002/zaac.201600313>
17. Cainelli, G.; Panunzio, M.; Andreoli, P.; Martelli, G.; Spunta, G.; Giacomini, D.; Bandini, E. *Pure & Appl. Chem.* **1990**, *62*, 605-612. DOI: <http://dx.doi.org/10.1351/pac199062040605>
18. Mladenova, R.; Ignatova, M.; Manolova, N.; Petrova, T.; Rashkov, I. *Eur. Polym. J.* **2002**, *38*, 989-999. DOI: [https://doi.org/10.1016/S0014-3057\(01\)00260-9](https://doi.org/10.1016/S0014-3057(01)00260-9)
19. Geindy-Mohamed, G.; Mohamed-Omar, M.; Mohamed-Hindy, A. *Turk. J. Chem.* **2006**, *30*, 361-382.
20. Shi, L.; Mao, W.-J.; Yang, Y.; Zhu, H.-L. *J. Coord. Chem.* **2009**, *62*, 3471-3477. DOI: <https://doi.org/10.1080/00958970903093694>
21. Mohamed, G.; Omar, M.; Ibrahim, A. *Spectrochim. Acta A Mol. Biomol. Spectrosc.* **2010**, *75*, 678-685. DOI: <https://doi.org/10.1016/j.saa.2009.11.039>
22. Razieh, A.; Mohammad, A.; Tahereh, S. *J. Mex. Chem. Soc.* **2014**, *58*, 173-179. DOI: <https://doi.org/10.29356/jmcs.v58i2.174>
23. Bathia, MS.; Mulani, AK.; Choudhari, PB.; Ingale, KB.; Bathia, NM. *Int. J. Drug. Discov.* **2009**, *1*, 1-9. DOI: <http://dx.doi.org/10.9735/0975-4423.1.1.1-9>
24. Yang, H.; Lou, C.; Sun, L.; Li, J.; Cai, Y.; Wang, Z.; Li, W.; Liu, G.; Tang, Y. *BMC Bioinform.* **2018**, *35*, 1067-1069. DOI: <https://doi.org/10.1093/bioinformatics/bty707>
25. admetsAR <http://lmmd.ecust.edu.cn/admetar2/> accessed in April **2021**
26. Daina, A.; Michelin, O.; Zoete, V. *J. Chem. Inf. Model.* **2014**, *54*, 3284-3301. DOI: <https://doi.org/10.1021/ci500467k>
27. Daina, A.; Zoete, V. *Chem. Med. Chem.* **2016**, *11*, 1117-1121. DOI: <https://doi.org/10.1002/cmdc.201600182>
28. Daina, A.; Michelin, O.; Zoete, V. *Sci. Rep.* **2017**, *3*, 42717. DOI: <https://doi.org/10.1038/srep42717>
29. SwissADME <http://www.swissadme.ch/> accessed in October **2020**
30. Peach, M.; Zakharov, A.; Liu, R.; Pugliese, A.; Tawa, G.; Wallqvist, A.; Nicklaus, M. *Future Med Chem.* **2012**, *4*, 1907-1932. DOI: <https://doi.org/10.4155/fmc.12.150>
31. Olsen, L.; Montefiori, M.; Phuc-Tran, K.; Steen-Jorgensen, F. *BMC Bioinform.* **2019**, *17*, 3174-3175. DOI: <https://doi.org/10.1093/bioinformatics/btz037>
32. SMARTCyp : Site of Metabolism prediction for Cytochrome P450s [https://smartcyp.sund.ku.dk/mol\\_to\\_som](https://smartcyp.sund.ku.dk/mol_to_som) accessed in April **2021**
33. ChemAxon-Marvin <https://chemaxon.com/products/marvin> accessed in April **2021**
34. Guan-Yeow, Y.; Sie-Tiong, H.; Nobuo, I.; Katsumi, S.; Peng-Lim, B.; Mahmood, B.; Ahmad, W. *J. Mol. Struct.* **2003**, *658*, 87-99. DOI: [https://doi.org/10.1016/S0022-2860\(03\)00453-8](https://doi.org/10.1016/S0022-2860(03)00453-8)
35. Mandal, S.; Rout, A.; Pilet, G.; Bandyopadhyay, D. *Transition. Met. Chem.* **2009**, *34*, 719-724. DOI: <https://doi.org/10.1007/s11243-009-9253-5>
36. Altomare, A.; Cascarano, G.; Giacovazzo, C.; Guagliardi, A. *J. Appl. Crystallogr.* **1993**, *26*, 343-350. DOI: <https://doi.org/10.1107/S0021889892010331>
37. Sheldrick, G. *Acta Cryst.* **2008**, *64*, 112-122. DOI: <https://doi.org/10.1107/S0108767307043930>
38. Spek, A. L. *Acta Cryst. D* **2009**, *65*, 148-155. DOI: <https://doi.org/10.1107/S090744490804362X>
39. Harada, J.; Harakawa, M.; Ogawa, K. *Acta Crystallogr. B.* **2004**, *60*, 578-588. DOI: <https://doi.org/10.1107/S0108768104016532>

40. These data can be obtained free of charge from the CCDC through the web page: <https://www.ccdc.cam.ac.uk/structures/> (CCDC 2046921)
41. Kiehlbauch, J.; Hannett, G.; Salfinger, M.; Archinal, W.; Monserrat, C.; Carlyn, C. *J Clin Microbiol.* **2000**, 38, 3341-3348. DOI: <https://doi.org/10.1128/JCM.38.9.3341-3348.2000>
42. Clinical and Laboratory Standards Institute (2017) Performance Standards for Antimicrobial Susceptibility Testing: 27<sup>th</sup> <https://webstore.ansi.org/standards/cls/clsim100s27> accessed in October **2020**
43. Clinical Laboratory Standards Institute (2018) Development of in vitro susceptibility testing criteria and quality controls parameters; approved guideline 5<sup>th</sup> ed. M23-Ed5E [https://www.techstreet.com/standards/cls-m23-ed5?product\\_id=2033354](https://www.techstreet.com/standards/cls-m23-ed5?product_id=2033354) accessed in October **2020**
44. Baron, E.J. *Classification. In Baron S. Medical microbiology*. 4<sup>th</sup> ed. Galveston (TX): University of Texas Medical Branch at Galveston. **1996**
45. Marques de Cantú, M.J. *Probabilidad y estadística para ciencias químico-biológicas*. McGraw-Hill, México. **1998**, 425-456, 471-486
46. Jaspers, S.; Aerts, M.; Verbeke, G.; Beloil, P-A. *Stat. Med.* **2014**, 33, 289-303. DOI: <https://doi.org/10.1002/sim.5939>
47. Nguyen, M.; Brettin, T.; Long, S-W.; Musser, J-M.; Olsen, R-J.; Olson, R.; Shukla, M.; Stevens, R.L.; Xia, F.; Yoo, H.; Davis, J-J. *Sci. Rep.* **2018**, 8, 1-11. DOI: <https://doi.org/10.1038/s41598-017-18972-w>
48. Liu, Y-Q.; Zhang, Y-Z.; Gao, P-J. *Antimicrob. Agents. Chemother.* **2004**, 48, 3884-3891. DOI: <https://doi.org/10.1128/AAC.48.10.3884-3891.2004>
49. Ren, S.; Wang, R.; Komatsu, K.; Bonaz-Krause, P.; Zyrianov, Y.; McKenna, C.; Csipke, C.; Tokes, Z.; Lien, E. *J. Med. Chem.* **2002**, 45, 410-419. DOI: <https://doi.org/10.1021/jm010252q>
50. Gertzen, C.; Gohlke, H. *Mol. Inform.* **2012**, 31, 698-704. DOI: <https://doi.org/10.1002/minf.201200015>
51. Ghose, AK.; Crippen, GM. *J. Chem. Informat. Model.* **1987**, 27, 21-35. DOI: <https://doi.org/10.1021/ci00053a005>
52. Morán Díaz, J.R.; Jiménez Vázquez, H.A.; Gómez Pliego, R.; Arellano Mendoza, M.G.; Quintana Zavala, D.; Guevara-Salazar, J.A. *Med. Chem. Res.* **2019**, 28, 1529-1546. DOI: <https://doi.org/10.1007/s00044-019-02391-9>
53. ACD/ChemSketch, Advanced Chemistry Development, Inc., Toronto, On, Canada, [www.acdlabs.com](http://www.acdlabs.com) accessed in September **2020**
54. Hansch, C.; Leo, A. *J. Pharm. Sci.* **1980**, 69, 1109 DOI: <https://doi.org/10.1002/jps.2600690938>
55. Hansch, C.; Fujita, T. *J. Am. Chem. Soc.* **1964**, 86, 1616-1626. DOI: <https://doi.org/10.1021/ja01062a035>
56. Williford, C.; Stevens, E. *QSAR. Comb. Sci.* **2004**, 23, 495-505. DOI: <https://doi.org/10.1002/qsar.200430863>
57. Alipour, M.; Safari, Z. *Chem. Phys.* **2016**, 18, 17917-17929. DOI: <https://doi.org/10.1039/C6CP02750D>
58. Schüürmann, G.; Ebert, R-U.; Chen, J.; Wang, B.; Kühne, R. *J. Chem. Inf. Model.* **2008**, 48, 2140-2145. DOI: <https://doi.org/10.1021/ci800253u>
59. Brunton, L.L.; Hida-Dandan, R.; Knollmann, B. Goodman & Gilman's: The Pharmacological Basis of Therapeutics, 13<sup>rd</sup> ed. United State of America. **2018**
60. Sultan, A.; Hoppenbrouwers, T.; Lemmens den, T.; Snijders, S.; van Neck, J.; Verbon, A.; de Maat, M.; van Wamel, W. *Infect. Immun.* **2019**, 87, 00605-00619. DOI: <https://doi.org/10.1128/IAI.00605-19>

61. Crousilles, A.; Maunders, E.; Bartlett, S.; Fan, C.; Ukor, E-F.; Abdelhamid, Y.; Baker, Y.; Floto, A.; Spring, D-R.; Welch, M. *Future Microbiol.* **2015**, 10, 1825-1836. DOI: <https://doi.org/10.2217/fmb.15.100>
62. Dewachter, L.; Verstraeten, N.; Fauvart, M.; Michiels, J. *FEMS Microbiol. Rev.* **2018**, 42, 116-136. DOI: <https://doi.org/10.1093/femsre/fuy005>
63. Berti, T.; Ferrari, M.; Galla, F.; Scuka, M. *Arch. Ital. Sci. Farmacol.* **1965**, 15, 203-208.
64. Bär H, Zarnack J. *Pharmazie.* **1970**, 25, 10-22.
65. Castillo-Vera, J.; Ribas-Aparicio, R-M.; Osorio-Carranza, L.; Aparicio, G. *Bioquímica.* **2006**, 17, 41-48.
66. Dudley, M-N.; Ambrose, P-G.; Bhavnani, S-M.; Craig, W-A.; Ferraro, M-J.; Jones, R-N. *Clin. Med. Microbiol.* **2013**, 56, 1301-1309. DOI: <https://doi.org/10.1093/cid/cit017>
67. Biedenbach, D-J.; Kazmierczak, K.; Bouchillon, S-K.; Sahm, D-F.; Brandford, P-A. *Antimicrob. Agents Chemother.* **2015**, 29, 4239-4248. DOI: <https://doi.org/10.1128/AAC.00206-15>